Available online at www.sciencedirect.com
SCIENCE DIRECT®
Journal of Solid State Chemistry 170 (2003) 58–67
JOURNAL OF SOLID STATE CHEMISTRY
http://elsevier.com/locate/jssc

Influence of titanium oxide on the surface interactions of *M*O (*M* = Cu and Ni)/γ-Al_2O_3 catalysts

Yuhai Hu, Tiandong Liu, Mingmin Shen, Haiyang Zhu, Shuting Wei, Xi Hong, Weiping Ding, Lin Dong,* and Yi Chen

Department of Chemistry, Nanjing University, Nanjing, 210093, China

Received 25 March 2002; received in revised form 20 June 2002; accepted 27 August 2002

Abstract

The influence of titanium oxide on the surface interactions of *M*O (*M* = Cu and Ni)/γ-Al_2O_3 catalysts has been studied by using XRD, LRS and XPS. For the catalysts with titania loadings lower than 0.56 mmol Ti^{4+}/100 m^2 Al_2O_3 (i.e., the dispersion capacity), the dispersion of *M*O oxides on the surface of γ-Al_2O_3 support is significantly suppressed by the dispersed Ti^{4+} ions. The inhibiting effect is dependent on the properties of *M*O oxides. When titania loadings are considerably higher than the dispersion capacity, *M*O oxides exhibit a rather stronger interaction with the formed TiO_2 particles than the γ-Al_2O_3 support, and some of the dispersed M^{2+} ions might be accommodated by the vacant sites on TiO_2. Therefore, the catalysts can be considered as the compositions of *M*O/TiO_2 and *M*O/TiO_2/γ-Al_2O_3 (dispersed titania). TPR results show that either dispersed titania or formed TiO_2 particles can promote the reduction of copper oxide species, but the latter to a greater extent. Based on the consideration of the incorporation model, it is proposed that the surface structure of the support plays an important role in surface interactions.

1. Introduction

It has been of increasing interest for the research and development of supported multi-component catalysts by modifying high-surface-area oxide supports with tetravalence metal oxides in the past years. In this respect, CuO/CeO_2/TiO_2 catalyst is studied for the complete oxidation of CO, ethanol, and ethyl acetate [1]; ZrO_2/γ-Al_2O_3 and ZrO_2/SiO_2 are studied for the reactions including hydrogenation of hydrocarbon, cracking, dehydrogenation [2,3]; MoO_3/TiO_2/γ-Al_2O_3 catalysts are studied for the hydro-desulfication reaction [4]. Importantly, NM (noble metal)/CeO_2/γ-Al_2O_3 catalysts are widely used for the elimination of automotive emission [5]. Recently, TiO_2/SiO_2, TiO_2–ZrO_2 and TiO_2–zeolites have also been widely investigated as potential supports for the catalyst preparation [6–8].

Generally, properties of such kind of catalysts are found to be strongly related to the doped metal oxides. These metal oxides can promote the dispersion of the active components, induce the creation of some new active sites, enhance the stability of supports in the course of high-temperature reaction, and in certain conditions, might also work as the active components, e.g., TiO_2 and ZrO_2 are the acid centers in the selective oxidation catalysts due to their relatively strong acidities [9].

Whereas some plausible researches have been carried out, there is still a lack of general agreement on the intrinsic mechanism of the surface interactions [10–12], and seldom are quantitative studies met. This might be due to: (I) many complex interactions resulted from the coexistence of multi-components, e.g., in CuO/CeO_2/γ-Al_2O_3 catalysts, the surface interactions involve dispersed copper oxide, crystalline CuO, dispersed ceria species, crystalline CeO_2 and γ-Al_2O_3 support; (II) coexistence of various crystalline planes with unknown ratios on the surface of powder oxide supports, which are too complicated to assess quantitatively.

Therefore, in the present work, dispersion capacities of copper (or nickel) oxide on the surface of

*Corresponding author. Present address: Laboratory of Surface Reaction Dynamics, Catalysis Research Center, Hokkaido University, Sapporo 060-0811, Japan.

E-mail addresses: yhhu0303@yahoo.com.cn (Y. Hu), chem718@netra.nju.edu.cn (L. Dong).

0022-4596/03/$ - see front matter © 2002 Elsevier Science (USA). All rights reserved.
PII: S0022-4596(02)00020-8

titania-modified γ-Al_2O_3 support are evaluated by modulating the titania loadings, and the reduction behaviors are also concerned. It is expected that this work will simplify the investigations on the multi-component catalysts and approach the knowledge about the intrinsic factors in the surface interactions.

2. Experimental

2.1. Sample preparation

A titania-modified γ-Al_2O_3 support (denoted as TiO_2/γ-Al_2O_3) was prepared by nonaqueous impregnation of γ-Al_2O_3 support (from Fusun Petrochemical Institute of China, with a BET surface area of 198 $m^2\,g^{-1}$ after pre-calcining in air at 700°C for 5 h.) with solutions of titanium (IV) isopropoxide, Ti(O-iPr)$_4$ (Acros Chemical Co.), dissolved in 2-propanol (A.R, Shanghai Chemical Plant), and the total amounts of solution was approximately equal to twice the pore volume of the support. Samples with titania loadings $\geqslant$0.7 mmol Ti^{4+}/100 m^2 Al_2O_3 were prepared by double impregnation of the support with half the amount of the titania precursor requisite at each step. Consequently, the samples were hydrolyzed in moist air at room temperature for 2 h and then dried under ambient condition for 48 h, followed by further drying in air at 120°C for 4 h. Finally, the impregnation samples were calcined at 500°C for 5 h.

The copper oxide supported samples ($CuO/TiO_2/\gamma$-Al_2O_3) were prepared by the incipient wetness impregnation of the TiO_2/γ-Al_2O_3 supports with aqueous solutions containing a requisite amount of $Cu(NO_3)_2$, the wet samples were dried in air at 100°C and then calcined in a flowing O_2 stream at 450°C for 5 h. The $NiO/TiO_2/\gamma$-Al_2O_3 samples were prepared in the method similar to that of $CuO/TiO_2/\gamma$-Al_2O_3, but with $Ni(NO_3)_2$ as the precursor. For the sake of simplicity, the samples are denoted as xCu(or Ni)-yTi-Al and the commonly used unit for the titania, copper oxide and nickel oxide loadings are employed, namely, millimole of Ti^{4+} (or Cu^{2+}, Ni^{2+}) per 100 m^2 of surface area of γ-Al_2O_3, e.g., 0.2Cu–0.7Ti–Al corresponds to the sample with copper oxide loading of 0.2 mmol Cu^{2+}/100 m^2 Al_2O_3 and titania loading of 0.7 mmol Ti^{4+}/100 m^2 Al_2O_3 respectively, and 0.2Cu–yTi–Al corresponds to the samples with copper oxide loading of 0.2 mmol Cu^{2+}/100 m^2 Al_2O_3 and various titania loadings.

2.2. Instruments

X-ray diffraction (XRD) patterns were obtained with a GEIGERAFLEX RAD diffractometer employing Cu$K\alpha$ radiation (0.15418 nm), the X-ray tube was operated at 40 kV and 60 mA, step width 0.02°. The BET surface areas were measured on a Micrometrics ASAP-2000 adsorption apparatus. FT-Raman spectra were taken on a Bruker RFS-100 Fourier transform spectrometer with Raman excitation at 1064 nm and a resolution of 4 cm^{-1}. X-ray photoelectron spectra (XPS) were recorded with a V.G. Escalab MK II system equipped with a hemispherical electron analyzer, an Mg$K\alpha$ anode was used, Al_{2p} binding energy value of 74.5 eV was used as a reference level.

A quantitative temperature programmed reduction (QTPR) analysis was carried out in a quartz U-tube reactor with 30 mg sample for each measurement. The sample was pretreated in an O_2 stream at 500°C for 1 h and then cooled to room temperature prior to an H_2-Ar mixture (7% H_2 by volume) being switched on. The temperature was increased linearly at a rate of 10°C/min. Before each measurement, a TPR profile of pure CuO (5 mg) was also obtained as a reference for the calculations.

3. Results

3.1. $CuO/TiO_2/\gamma$-Al_2O_3 samples

3.1.1. XRD results

The appearance of the diffraction peaks of crystalline CuO is observed to be related to copper oxide and titania loadings. For the samples of xCu–0.13Ti–Al, the peaks appear as copper oxide loadings are increased to 0.6 mmol Cu^{2+}/100 m^2 Al_2O_3 ($2\theta = 35.5°$, 38.7°, 48.7°, etc.), and the peak intensities are also increased with increasing copper oxide loadings, in Fig. 1. For the samples of xCu–0.40Ti–Al and xCu–0.70Ti–Al, the peaks are observed as the copper oxide loadings reach 0.2 mmol Cu^{2+}/100 m^2 Al_2O_3, as shown in line (a) of Figs. 2 and 3, respectively. When the titania loading is increased to 1.21 mmol Ti^{4+}/100 m^2 Al_2O_3, the peaks

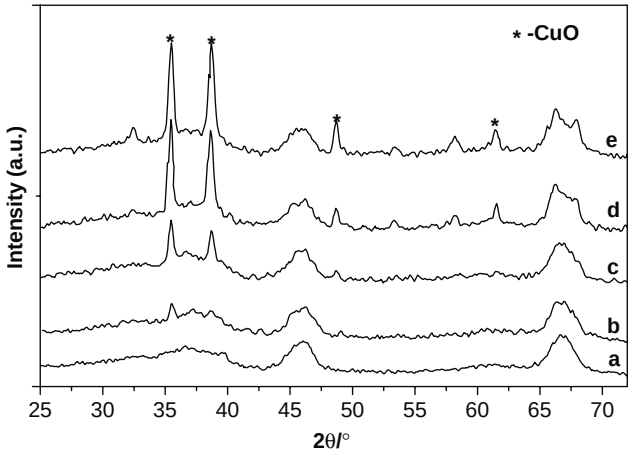

Fig. 1. XRD patterns of xCu–0.13Ti–Al samples with copper oxide loadings of (a) 0.2, (b) 0.6, (c) 0.8, (d) 1.2 and (e) 1.6 mmol Cu^{2+}/100 m^2 Al_2O_3.

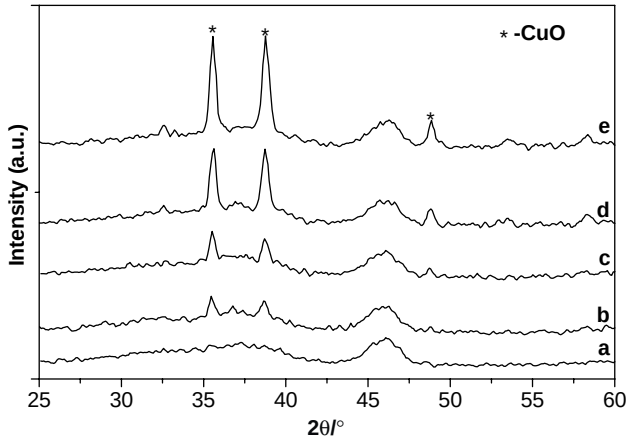

Fig. 2. XRD patterns of xCu–0.40Ti–Al samples with copper oxide loadings of (a) 0.2, (b) 0.6, (c) 0.8, (d) 1.2 and (e) 1.6 mmol Cu^{2+}/100 $m^2 Al_2O_3$.

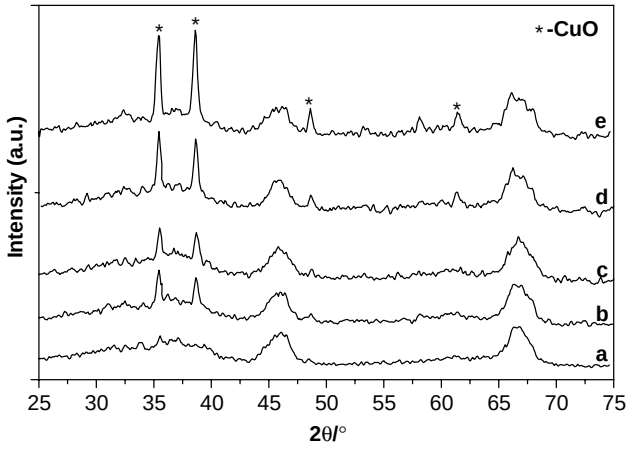

Fig. 3. XRD patterns of xCu–0.70Ti–Al samples with copper oxide loadings of (a) 0.2, (b) 0.6, (c) 0.8, (d) 1.2 and (e) 1.6 mmol Cu^{2+}/100 $m^2 Al_2O_3$.

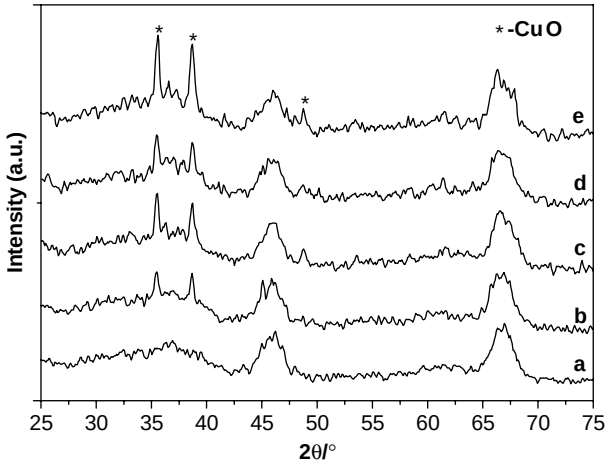

Fig. 4. XRD patterns of xCu–1.21Ti–Al samples with copper oxide loadings of (a) 0.2, (b) 0.6, (c) 0.8, (d) 1.2 and (e) 1.6 mmol Cu^{2+}/100 $m^2 Al_2O_3$.

appear in the sample with copper oxide loading of 0.6 mmol Cu^{2+}/100 m^2 Al_2O_3, in Fig. 4.

A quantitative analysis is carried out by measuring the peak intensity ratios of crystalline CuO and γ-Al_2O_3 support as a function of copper oxide loadings [13], the results are listed in Table 1. Initially, the dispersion capacities of copper oxide are decreased with increasing titania loadings, but when titania loadings are up to 1.21 mmol Ti^{4+}/100 m^2 Al_2O_3, the dispersion capacity is increased to 0.15 mmol Cu^{2+}/100 m^2 Al_2O_3. Accordingly, it can be deduced that the doped titania species have a considerably strong influence on the dispersion of copper oxide on the surface of γ-Al_2O_3.

3.1.2. XPS results

XPS experiments are carried out for 0.6Cu–yTi–Al samples. The binding energies of Cu_{2p} shift downward clearly with increasing titania loadings as shown in Fig. 5. In sample 0.6Cu–0.13Ti–Al, the peak maximum is at 934.2 eV, while in sample 0.6Cu–1.21Ti–Al, the peak maximum is about 933.4 eV. Recalling the previous studies, the former corresponds to Cu^{2+} ions dispersed

Table 1
Dispersion capacities of copper oxide on different titania-modified γ-Al_2O_3 support

Samples	Titania loadings (mmol Ti^{4+}/100 m^2 Al_2O_3)	Dispersion capacity (mmol Cu^{2+}/100 $m^2Al_2O_3$)
xCu–0.13Ti–Al	0.13	0.58
xCu–0.40Ti–Al	0.40	0.14
xCu–0.70Ti–Al	0.70	—
xCu–1.21Ti–Al	1.21	0.15

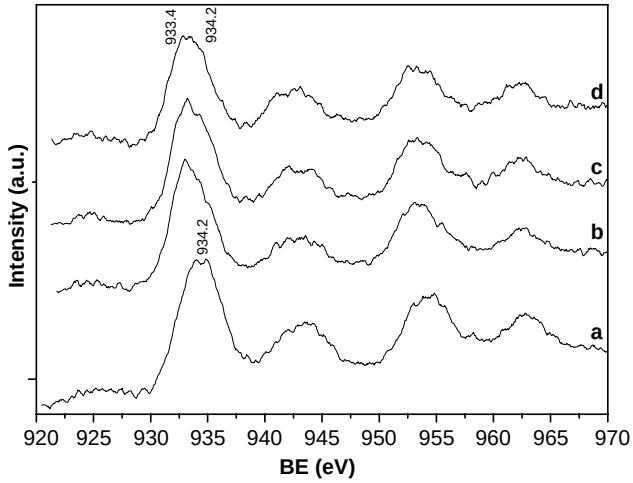

Fig. 5. $Cu2p_{3/2}$ XPS results for 0.6Cu–yTi-Al samples with titania loadings of (a) 0.13, (b) 0.4, (c) 0.7 and (d) 1.21 mmol Ti^{4+}/100 $m^2Al_2O_3$.

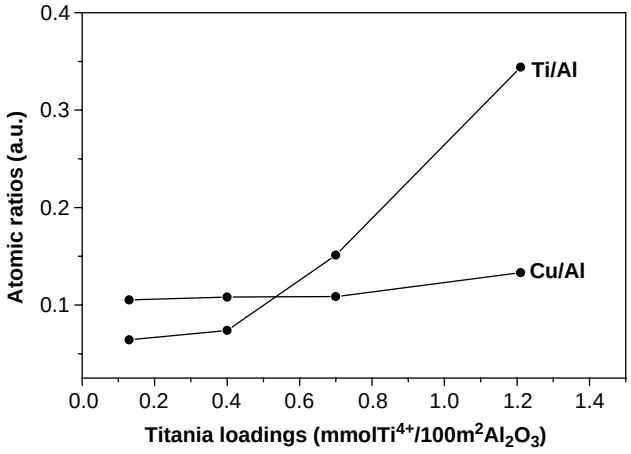

Fig. 6. Surface atomic ratios from XPS measurement as a function of titania loadings for the 0.6Cu–yTi–Al samples.

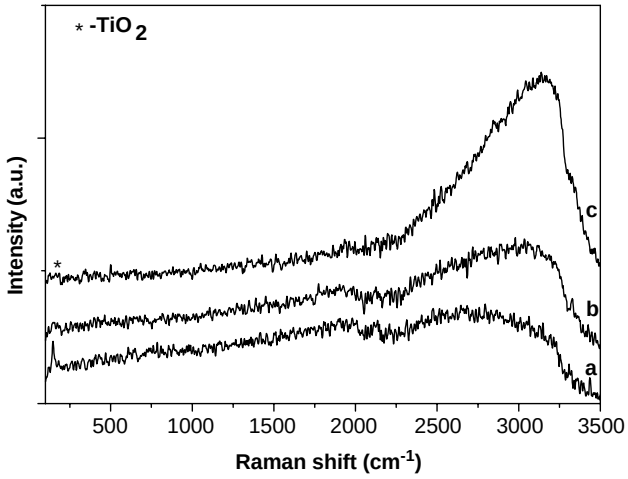

Fig. 7. Raman spectra for the xCu–1.21Ti–Al samples with copper oxide loadings of (a) 0.2, (b) 0.4 and (c) 0.6 mmol $Cu^{2+}/100\,m^2Al_2O_3$.

on the surface of γ-Al_2O_3 support [14], the latter corresponds to copper oxide (Cu^{2+}) which strongly interacts with TiO_2 particles, respectively [15]. Since XPS is surface sensitivity, the binding energy difference indicates that the states of copper oxide species are changed along with increasing titania loadings.

Fig. 6 shows the surface atomic ratios of Cu (or Ti) and Al via titania loadings. It can be seen that the surface Cu/Al atomic ratios are not changed evidently. However, the surface Ti/Al atomic ratios are increased significantly as titania loadings are beyond 0.4 mmol $Ti^{4+}/100\,m^2$ Al_2O_3, which means that TiO_2 particles have been formed in these samples. Recently, some workers have been trying to deduce the information on the particle shapes and sizes of the active components in the supported catalysts by measuring the peak intensity ratios. Generally, it is believed that the variation of the intensity ratio is caused by the formation of new phase in the catalyst [16,17].

3.1.3. Raman results

Raman spectra of xCu–1.21Ti–Al samples are shown in Fig. 7. The appearance of the peak at 144 cm^{-1} indicates that TiO_2 particles (Anatase) are formed in these samples, which is well consistent with the results from XPS. It is worth noting that the peak intensities are decreased steadily with increasing copper oxide loadings, and disappear in sample 0.6Cu–1.2Ti–Al, as seen by comparing Fig. 7b and c. As reported elsewhere [18], dispersed copper oxides species can suppress the Raman signals of TiO_2 support in the CuO/TiO_2 catalysts. In addition, we have also reported that copper oxide species can induce the Raman intensity decrease of the ceria species either as dispersed phase or mixture with crystalline CeO_2 [19], but the influence of the former species is much greater than the latter one. Like copper oxide, the deposition of vanadium and molybdenum

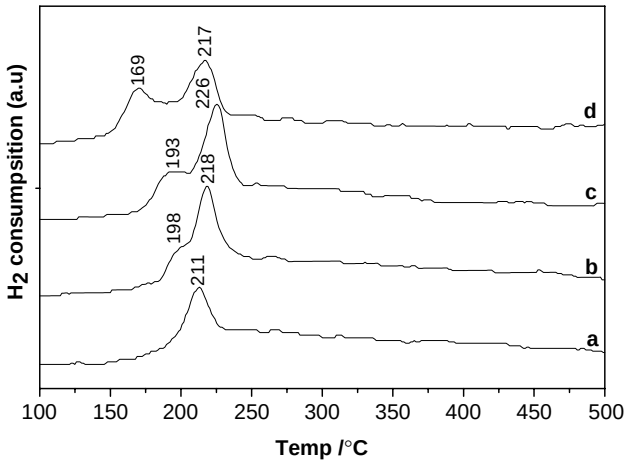

Fig. 8. TPR profiles for the 0.2Cu-yTi-Al samples with titania loadings of (a) 0.13, (b) 0.4, (c) 0.7 and (d) 1.21 mmol $Ti^{4+}/100\,m^2Al_2O_3$.

oxides on the surfaces of TiO_2 or ZrO_2 has also been found to suppress the Raman intensities of the oxide supports [20,21]. Therefore, it might be concluded that the change of Raman intensity is probably due to the coexistence of dispersed copper oxide species and the formed TiO_2 particles.

3.1.4. TPR results

0.2Cu–yTi–Al samples. TPR profiles of 0.2Cu–yTi–Al samples are shown in Fig. 8. For sample 0.2Cu–0.13Ti–Al, only one peak with hydrogen consumption maximum centered at 211°C is observed. On increasing titania loading to higher values, two reduction peaks appear, and the peak maximums are changed significantly with titania loadings, as seen by comparing lines b–d in Fig. 8. The quantitative TPR result in Table 2 shows that the amounts of the lower-temperature copper oxide species are increased with titania loadings.

Table 2
Quantitative TPR results for the $CuO/TiO_2/\gamma$-Al_2O_3 samples

Samples	Peak-1 (°C)	Peak-2 (°C)	Peak-3 (°C)	Intensity ratios (a.u.)
0.2Cu–0.13Ti–Al		211		—-
0.2Cu–0.40Ti–Al	198	218		0.2
0.2Cu–0.70Ti–Al	193		226	0.4
0.2Cu–1.21Ti–Al	169		217	0.7
0.6Cu–0.13Ti–Al		212	230	2.3
0.6Cu–0.40Ti–Al		203	236	1.0
0.6Cu–0.70Ti–Al	185		234	0.6
0.6Cu–1.21Ti–Al	176		233	1.4
1.2Cu–0.13Ti–Al		202	235	0.2
1.2Cu–0.40Ti–Al	183		235	0.5
1.2Cu–0.70Ti–Al	164		232	1.1
1.2Cu–1.21Ti–Al	165		227	1.5

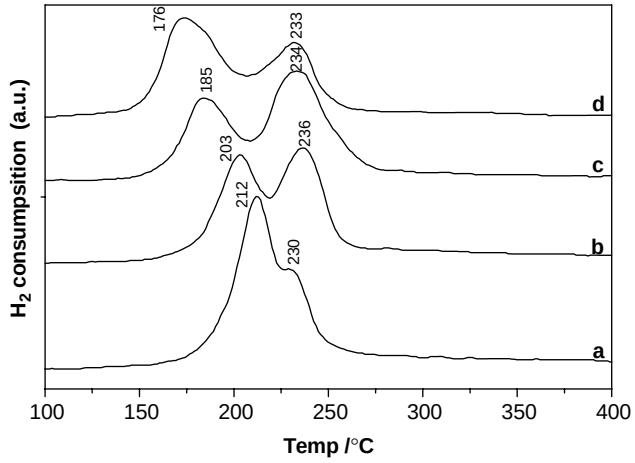

Fig. 9. TPR profiles for the 0.6Cu-yTi-Al samples with titania loadings of (a) 0.13, (b) 0.4, (c) 0.7 and (d) 1.21 mmol $Ti^{4+}/100\,m^2Al_2O_3$.

0.6Cu-yTi-Al samples TPR profiles for the 0.6Cu–yTi–Al samples are shown in Fig. 9. Two peaks are observed in the whole titania loading regime, but the peak shapes and hydrogen consumption maximums differ significantly. The lower-temperature peak at 212°C for sample 0.6Cu–0.13Ti–Al shift steadily downward, i.e., 176°C for sample 0.6Cu–1.21Ti–Al. The higher-temperature (at about 230°C) peaks did not shift evidently. The peak intensity ratios are also changed in a rather different way as compared to those for the 0.2Cu–yTi–Al samples. The ratios are decreased from 2.34 to 0.62 as titania loadings are increased from 0.13 to 0.70 mmol $Ti^{4+}/100\,m^2$ Al_2O_3. However, when titania loadings are increased to 1.21 mmol $Ti^{4+}/100\,m^2$ Al_2O_3, the ratios are increased to 1.42, as listed in Table 2.

1.2Cu-yTi-Al samples. For sample 1.2Cu–0.13Ti–Al, a strong reduction peak with a weak shoulder appears, and when titania loadings are increased to 0.40 mmol $Ti^{4+}/100\,m^2$ Al_2O_3, two peaks centered at 183°C and 235°C are observed. As titania loadings are increased to

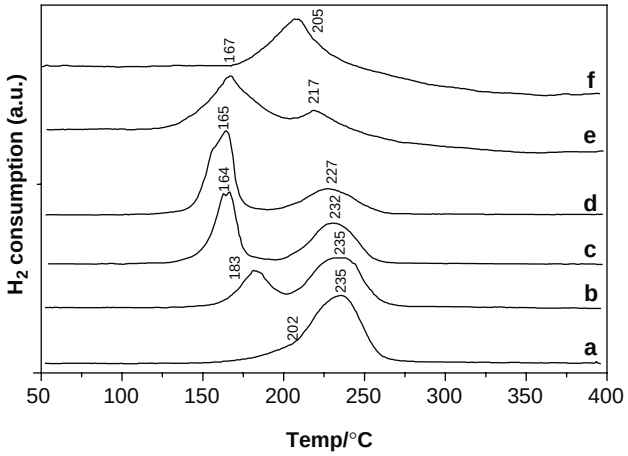

Fig. 10. TPR profiles for the 1.2Cu–yTi–Al samples with titania loadings of (a) 0.13, (b) 0.4, (c) 0.7 and (d) 1.21 mmol $Ti^{4+}/100\,m^2Al_2O_3$, (e) CuO/TiO_2, and (f) CuO/γ-Al_2O_3.

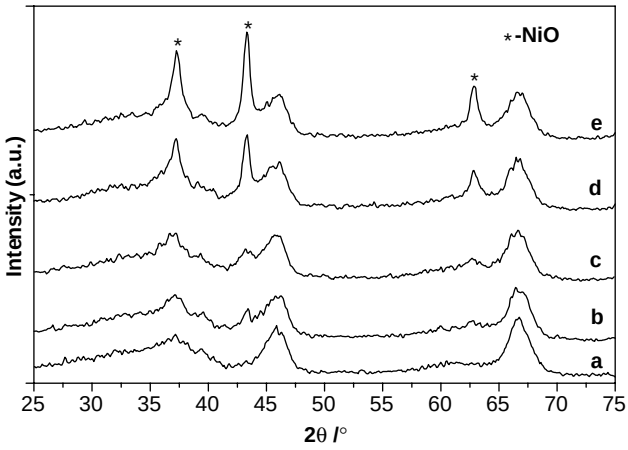

Fig. 11. XRD patterns of xNi–0.55Ti–Al sampleswith nickel oxide loadings of (a) 0.4, (b) 0.8, (c) 1.2, (d) 1.6, and (e) 2.0 mmol $Ni^{2+}/100\,m^2Al_2O_3$.

0.7 and 1.2 mmol $Ti^{4+}/100\,m^2$ Al_2O_3, the lower-temperature peak shifts to about 165°C, as shown in Fig. 10. Moreover, the amounts of the lower-temperature-reduction copper oxide species are increased continuously with titania loadings, which can be seen in Table 2.

3.2. $NiO/TiO_2/\gamma$-Al_2O_3 samples

Shown in Fig. 11 are the XRD patterns of xNi–0.55Ti–Al samples, the typical diffraction peaks corresponding to crystalline NiO are observed for the samples with nickel oxide loadings higher than 0.4 mmol $Ni^{2+}/100\,m^2$ Al_2O_3. Measured peak intensity ratios of crystalline NiO (centered at 43.3°) and γ-Al_2O_3 support (centered at 66°) indicate that the dispersion capacity of nickel oxide on this titania-modified support is about 0.42 mmol $Ni^{2+}/100\,m^2$ Al_2O_3, as shown in Fig. 12.

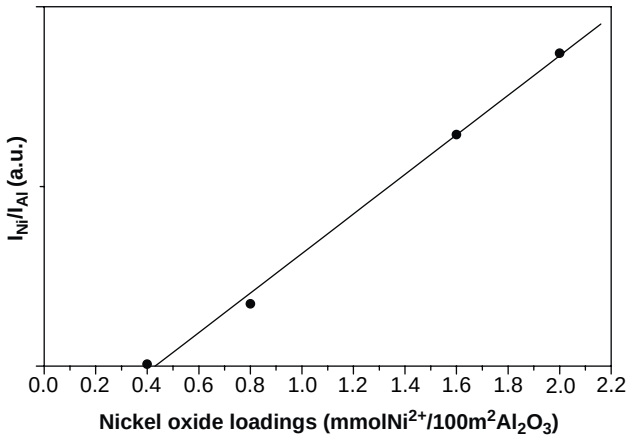

Fig. 12. Quantitative XRD results for the *x*Ni–0.55Ti–Al samples.

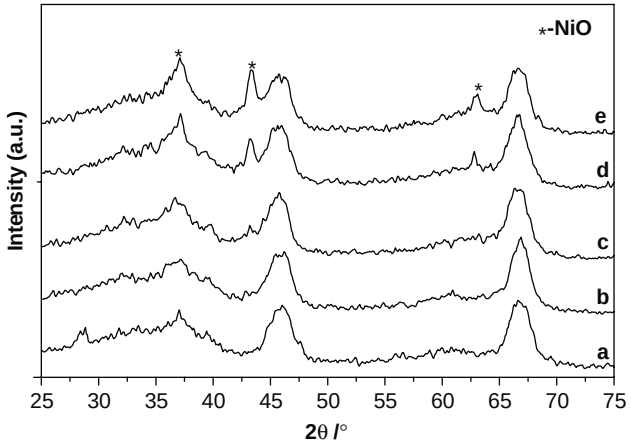

Fig. 13. XRD patterns of *x*Ni–1.03Ti–Al catalysts with nickel oxide loadings of (a) 0.2, (b) 0.4, (c) 0.8, (d) 1.2, and (e) 1.6 mmol Ni^{2+}/100 $m^2Al_2O_3$.

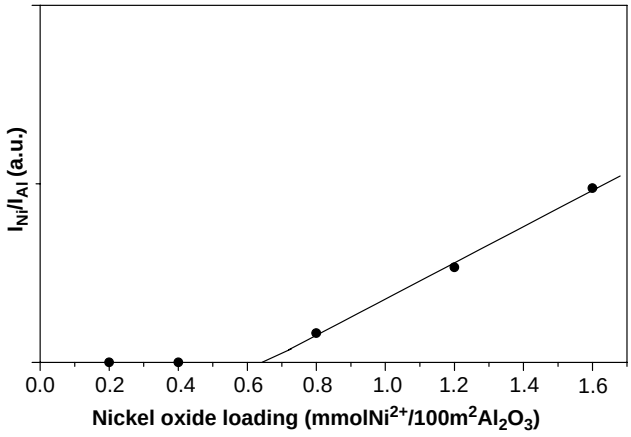

Fig. 14. Quantitative XRD results for the *x*Ni–1.03Ti–Al samples.

When titania loadings are increased to 1.03 mmol Ti^{4+}/100 m^2 Al_2O_3, the diffraction peaks of crystalline NiO appear in the sample with a nickel oxide loading of 0.8 mmol Ni^{2+}/100 m^2 Al_2O_3, as shown in Fig. 13. Quantitative XRD results indicate that the dispersion capacity of nickel oxide species on this titania-modified support is 0.64 mmol Ni^{2+}/100 m^2 Al_2O_3, as shown in Fig. 14. It thus might be concluded that the dispersion behaviors of the nickel oxide on the titania-modified γ-Al_2O_3 supports are also strongly related to titania loadings.

4. Discussion

4.1. Surface states of titania species on γ-Al_2O_3

The foregoing XRD, XPS, Raman and TPR results clearly demonstrate that predoped titania species on the surface of γ-Al_2O_3 significantly influence the surface interactions between copper (or nickel) oxide and γ-Al_2O_3 support. Therefore, to approach the surface interactions in these multi-component catalyst systems, it might be more profitable to study the surface interactions between titania and γ-Al_2O_3 as the first attempt.

γ-Al_2O_3 can be assumed to consist of particles formed by one-dimension stacking of C- and D-layers. For this oxide, (110) and (100) planes are preferentially exposed [22], on which octahedral and tetrahedral sites are formed. Based on the consideration of incorporation model [23], when titania species are dispersed on the surface of γ-Al_2O_3, Ti^{4+} ions are proposed to occupy the surface octahedral sites, and two oxygen anions associating with Ti^{4+} ion will cap over for charge compensation. It should be noted that although each dispersed Ti^{4+} can only occupy one octahedral site, due to the capping effect of oxygen, some of the neighboring octahedral sites are not available for the occupation of Ti^{4+}. Fig. 15 shows the schematic diagram for the dispersed titania species on the (110) plane of γ-Al_2O_3, in which it can be seen that two adjacent octahedral sites are occupied by a dispersed TiO_2 "molecular". Statistically, $2Ti^{4+}$ ions could be incorporated into one unit mesh (each unit mesh is 0.443 nm^2, based on the radius of O^{2-} ion being 0.14 nm) of the D-layer, and one Ti^{4+} could be incorporated into one unit mesh of the C-layer. Considering that the exposed possibilities of C- and D-layer are equal, it can be assumed that the dispersion capacity of titania on the surface of γ-Al_2O_3 is 0.55 mmol Ti^{4+}/100 m^2 Al_2O_3. This result is in good agreement with that reported in literature [24]. Providing that the loadings are below the dispersion capacity, titania species will be dispersed on the surface of the γ-Al_2O_3 in the way described above, and after the usable sites are occupied, the capping oxygen anions form an epitaxial layer on the top of γ-Al_2O_3 surface. In case titania loadings are highly beyond the dispersion capacity, the remaining titania species will form TiO_2

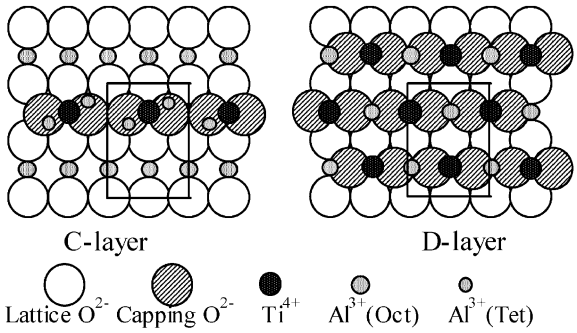

Fig. 15. Schematic diagram for the dispersed titania species on the (110) plane of γ-Al_2O_3.

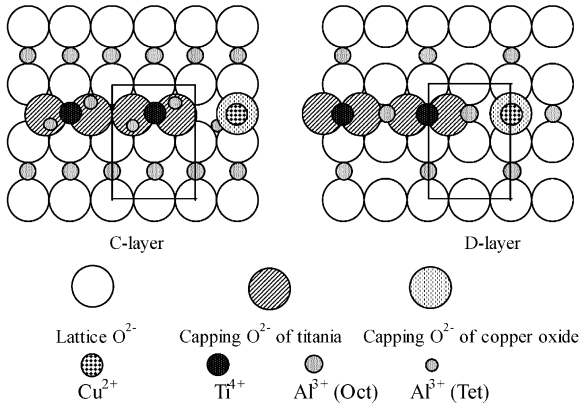

Fig. 16. Schematic diagram for the dispersion of copper oxide species on the titania-modified γ-Al_2O_3.

particles, which will grow up with increasing titania loadings, and the modified support can be considered as the mixture of TiO_2 and TiO_2/γ-Al_2O_3.

4.2. States of copper oxides on the titania-modified γ-Al_2O_3 supports

Dispersion of copper oxide species on the surface of γ-Al_2O_3 has always been of interest in catalysis and surface science, and well investigated by using various techniques [25,26]. It has been acknowledged that the dispersion capacity of copper oxide on γ-Al_2O_3 is about 0.75 mmol $Cu^{2+}/100\,m^2$ Al_2O_3, and the dispersed Cu^{2+} ions are suggested to occupy the surface octahedral sites of γ-Al_2O_3 support due to its specific electric structure [13,27,28]. Consequently, it is reasonable to rationalize the influence of titania species in view of the occupation of surface sites by the dispersed Ti^{4+}.

Shown in Fig. 16 is the schematic diagram for the dispersion of copper oxide on the titania-modified γ-Al_2O_3 support. When titania loading is 0.13 mmol $Ti^{4+}/100\,m^2$ Al_2O_3, supposing that the dispersed Ti^{4+} ions totally occupy the sites on C-layer, the concentration of surface octahedral sites occupied is about 0.26 mmol/$100\,m^2$ Al_2O_3, and the concentration of the available sites for the dispersion of copper oxide species on this modified layer is about 0.49 mmol/$100\,m^2$ Al_2O_3, i.e., dispersion capacity of copper oxide species. On the other hand, if titania species are preferentially dispersed on D-layer, due to the capping O^{2-} having no effect on the neighboring octahedral sites, the dispersion capacity of copper oxide is about 0.62 mmol $Cu^{2+}/100\,m^2$ Al_2O_3. Taking the exposed possibilities of the two layers into consideration, on the theoretical grounds, the dispersion capacity of copper oxide on the titania-modified γ-Al_2O_3 support with titania loading of 0.13 mmol $Ti^{4+}/100\,m^2$ Al_2O_3 is 0.56 mmol $Cu^{2+}/100\,m^2$ Al_2O_3, which is basically in agreement with the value calculated by quantitative XRD.

When titania loadings are increased to 0.40 mmol $Ti^{4+}/100\,m^2$ Al_2O_3, the conditions are relatively complex. Supposing that dispersed titania preferentially occupy the sites on C-layer, there will be no vacant octahedral sites available, and copper oxide species can hardly be dispersed on this modified layer. For the case of D-layer, the dispersion capacity of copper oxide is about 0.35 mmol $Cu^{2+}/100\,m^2$ Al_2O_3. Statistically, the dispersion capacity of copper oxide species on this modified support is about 0.18 ($0\times 50\% + 0.35\times 50\% = 0.18$), this value is still identical to the results from quantitative XRD.

As the titania loadings are increased slightly beyond the dispersion capacity, either on C-layer or on D-layer, there are no effective available vacant sites for Cu^{2+} ions. So, dispersion capacity of copper oxide on the titania-modified γ-Al_2O_3 with titania loading of 0.7 mmol $Ti^{4+}/100\,m^2$ Al_2O_3 is zero. However, when titania loadings are highly beyond the dispersion capacity, theoretically, the modified-support can be considered as the mixture of TiO_2/γ-Al_2O_3 and TiO_2 particles as suggested above. The formed TiO_2 particles give rise to some new vacant sites [29], which can also accommodate the dispersed Cu^{2+} ions. This might be the reason why the dispersion capacity of copper oxide is increased to 0.15 mmol $Cu^{2+}/100\,m^2$ Al_2O_3 when titania loadings are increased to 1.2 mmol $Ti^{4+}/100\,m^2$ Al_2O_3, as compared to that with titania loading of 0.7 mmol $Ti^{4+}/100\,m^2$ Al_2O_3.

Based on the above discussion, copper oxide species in the $CuO/TiO_2/\gamma$-Al_2O_3 catalysts can be assumed to be in the following forms: dispersed copper oxide species on the surface of γ-Al_2O_3 (denoted as Cu-I), very small CuO particles intimately interact with the surface dispersed titania or TiO_2 particles (denoted as Cu-II), dispersed copper oxide species on the surface of the formed TiO_2 particles (denoted as Cu-III), CuO particles interact with γ-Al_2O_3 support (denoted as Cu-IV), details are summarized in Table 3. Comprehensively, the amounts of the above copper oxide species are closely related to titania loadings.

Table 3
Suggested copper oxide species in $CuO/TiO_2/\gamma$-Al_2O_3 samples

Samples	Copper oxide species			
0.2Cu–0.13Ti–Al	Cu-I	Cu-II		
0.2Cu–0.40Ti–Al	Cu-I	Cu-II		Cu-IV
0.2Cu–0.70Ti–Al		Cu-II		Cu-IV
0.2Cu–1.21Ti–Al		Cu-II	Cu-III	Cu-IV
0.6Cu–0.13Ti–Al	Cu-I	Cu-II		Cu-IV
0.6Cu–0.40Ti–Al	Cu-I	Cu-II		Cu-IV
0.6Cu–0.70Ti–Al		Cu-II		Cu-IV
0.6Cu–1.21Ti–Al		Cu-II	Cu-III	Cu-IV
1.2Cu–0.13Ti–Al	Cu-I	Cu-II		Cu-IV
1.2Cu–0.40Ti–Al	Cu-I	Cu-II		Cu-IV
1.2Cu–0.70Ti–Al		Cu-II		Cu-IV
1.2Cu-1.21Ti–Al		Cu-II	Cu-III	Cu-IV

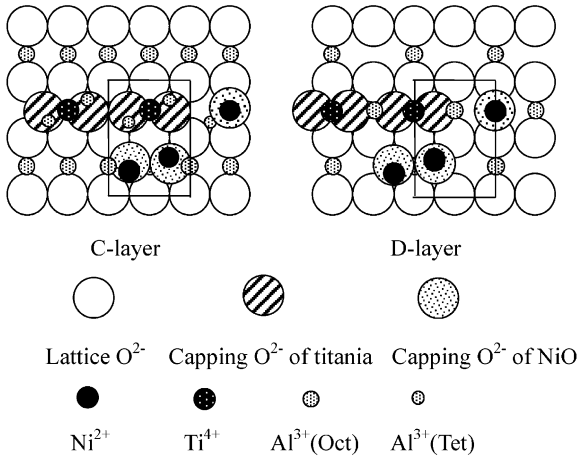

Fig. 17. Schematic diagram for the dispersion of nickel oxide species on the titania-modified γ-Al_2O_3.

4.3. States of nickel oxides on the titania-modified γ-Al_2O_3 supports

By comparing the quantitative XRD results, it can be seen that the dispersion capacities of nickel oxide on the titania-modified γ-Al_2O_3 supports are higher than those of copper oxide, whereas the amounts of surface-dispersed titania species in the $NiO/TiO_2/\gamma$-Al_2O_3 samples are higher than the latter ones. This difference is probably originated from the different surface interactions in the CuO/γ-Al_2O_3 and NiO/γ-Al_2O_3 systems.

For the NiO/γ-Al_2O_3 sample, it has been established that at lower temperature calcinations, dispersed Ni^{2+} will preferentially occupy the surface tetrahedral sites of γ-Al_2O_3, although the octahedral sites can also be occupied. Thus, the dispersion capacity of nickel oxide on the surface of γ-Al_2O_3 has been proved to be about 1.51 mmol $Ni^{2+}/100\,m^2$ Al_2O_3 [13], which is higher than that of copper oxide. For the case of titania-modified γ-Al_2O_3 support with a titania loading of 0.56 mmolTi^{4+}/$100\,m^2Al_2O_3$, although the dispersed Ti^{4+} does not occupy the tetrahedral sites, it is inevitable that some of these sites are not accessible for the dispersed Ni^{2+} ions due to the capping effect of the dispersed titania species, as shown in Fig. 17. So, on D-layer, both octahedral and tetrahedral sites have been completely occupied by the dispersed Ti^{4+}, there are no available sites for the occupation of Ni^{2+} ions. While on C-layer, all the octahedral sites are occupied, there are two tetrahedral sites available in each of the unit meshes, corresponding to the site concentration of 0.75 mmol/$100\,m^2$ Al_2O_3. Considering the exposed possibility of C-layer as 50%, the dispersion capacity of nickel oxide on this modified support is estimated to be 0.38 mmol $Ni^{2+}/100\,m^2$ Al_2O_3. This value is consistent with the results from the XRD, i.e., 0.42 mmol $Ni^{2+}/100\,m^2$ Al_2O_3.

When titania loadings are increased to 1.03 mmol $Ti^{4+}/100\,m^2$ Al_2O_3, the dispersion capacity of nickel oxide species is about 0.64 mmol $Ni^{2+}/100\,m^2$ Al_2O_3, which is larger than that expected, i.e., 0.38 mmol Ni^{2+}/ $100\,m^2$ Al_2O_3. This difference can also be attributed to the contribution of the formed TiO_2 particles, as have been discussed for $CuO/TiO_2/\gamma$-Al_2O_3 samples.

The above considerations are supported by Hercules et al. [24], who, in 1980s, reported their research on the relationships between surface states of cobalt oxide and titania loadings in the CoO_x/TiO_2-γ-Al_2O_3 catalysts (3 wt% of Co, corresponding to 0.29 mmol Co/$100\,m^2$ Al_2O_3). They found that when the titania loadings are lower than 4 wt% of Ti (corresponding to 0.49 mmol Ti/ $100\,m^2$ Al_2O_3), the XRD spectra only show peaks of Co_3O_4, while when titania loadings are increased to 1.8 mmol Ti/$100\,m^2$ Al_2O_3, the peaks of crystalline Co_3O_4 can hardly be seen. Although there are no quantitative studies, the contribution of TiO_2 particles to the dispersion of cobalt oxide is basically similar to our present results.

4.4. Influence of tinania on the reduction of copper oxide species

For studying the influence of tinania on the reduction of copper oxide species, it is of interest first to briefly summarize some earlier TPR results for CuO/TiO_2 samples. Larsson et al. have attributed the copper oxide species on the surface of TiO_2 to three forms, i.e., monomeric dispersed copper oxide, polymeric copper oxide, and bulk CuO [18]. The former two types of copper oxide species strongly interact with the TiO_2 support, while the polymeric copper oxide, which forms patches or bidimensional layer on the support, is more reducible than the monomeric species. Sermon et al. [30], from XPS and TPR measurements, recorded two reduction peaks during the reduction of CuO/TiO_2 systems that were related to the reduction of well and poorly dispersed Cu^{2+} species, respectively, instead of a

two-step reduction $Cu^{2+} \rightarrow Cu^{+} \rightarrow Cu$. Del Arco ascribed the copper oxide species on the surface of TiO_2 to cluster CuO and well-dispersed Cu^{2+} [31]. Considering the complexity of copper oxide reduction on the surface of TiO_2, the present paper will not concentrate on the assignments of the reduction peaks in $CuO/TiO_2/\gamma$-Al_2O_3 samples, but mainly concern with the influence of the doped titania species on the reduction of the copper oxide species.

By comparing the TPR profiles of $CuO/TiO_2/\gamma$-Al_2O_3 samples, it can be clearly seen that the doped titania species promote the reduction of copper oxide species. The more the titania is loaded, the lower values the lower-temperature peaks shift to. The results also indicate that TiO_2 support can enhance the reduction of copper oxide species to a much greater extent as compared to γ-Al_2O_3, as have been shown in lines (e) and (f) in Fig. 10. The influence of the support on the reduction behaviors of copper oxide species is well studied, and some explanations are also presented [32,33]. Probably, for the two supports in this work, the electric properties differences are assumed to be the central determinant of the surface interactions as well as the reduction properties of copper oxide species. TiO_2 is an n-type semiconductor, while γ-Al_2O_3 is an insulator, the strengths of the Cu–TiO_2 are predicted to be stronger than γ-Al_2O_3 [34]. As a consequence, it can be proposed that the copper oxide species (either dispersed or bulk CuO) on the titania-modified γ-Al_2O_3 supports will have a preference to localize in the titania-rich region, and show the ease of H_2 reduction, which can be seen by comparing the peak ratios. This suggestion is strongly promoted by the studies of Fernadez-Garcia et al. [35], who have reported that in the $CuO/CeO_2/\gamma$-Al_2O_3 catalysts, the copper oxide species shows a preferential nucleation in the ceria-rich region, leading to a particle size smaller than the γ-Al_2O_3-supported system, and the reducibility of the copper oxide species are significantly enhanced. Although they did not relate this result to the conducting properties of ceria, essentially, ceria can also be regarded as a semiconductor.

However, it should be emphasized that, although copper oxide species in the $CuO/TiO_2/\gamma$-Al_2O_3 have been assigned in the foregoing part of this paper, the interpretation about the reduction peaks is very gross, and it might be too arbitrary to ascribe the reduction peaks to a certain state of copper oxide species; many issues contributing to the reduction of copper oxide species, e.g., particle sizes of TiO_2 and CuO. Essentially, for the modified catalysts, it is necessary to modulate titania loading, because in case titania loadings are highly beyond the dispersion capacity, TiO_2 particles are formed, on which copper oxide will aggregate, and the catalysts will show some properties just like those of the CuO/TiO_2 catalysts. This kind of catalysts can show some more positive activities as compared to CuO/γ-Al_2O_3, but some drawbacks will also generate as have been observed in the CuO/TiO_2 catalysts. Huang et al. also addressed this problem in their studies on Pt–Rh/TiO_2/Al_2O_3 catalysts [36].

5. Conclusion

Dispersion of di-valence metal oxides on the surface of titania-modified γ-Al_2O_3 supports is not only strongly correlated to titania loadings but also to the intrinsic properties of the metal oxides. The dispersed titania species are found to inhibit the dispersion of di-valence metal oxides by the occupation of the surface octahedral sites of γ-Al_2O_3 support with Ti^{4+} ions, but the inhibition effects are different for copper and nickel oxides. When tiania loadings are highly beyond the dispersion capacity, although all the octahedral sites are occupied, copper and nickel oxide species can also be accommodated in the surface sites of the formed TiO_2 particles, which contribute to the increasing dispersion capacities of the two oxides. Either dispersed titania or TiO_2 particles greatly promote the reduction of copper oxide species, while the influence of TiO_2 particles is to a larger extent. Essentially, it is necessary to monitor titania loadings for the modified catalysts to sustain a high-temperature stability.

References

[1] P. Larsson, A. Andersson, J. Catal. 179 (1998) 72, doi:10.1006/jcat.1998. 2198.
[2] Z. Dang, B.G. Anderson, Y. Amenomiya, B.A. Morrow, J. Phys. Chem. 99 (1995) 14437.
[3] S. Damyanova, P. Grange, B. Delmon, J. Catal. 168 (1997) 421, doi:10.1006/jcat.1997. 1671.
[4] Z. Wei, H. Zhang, Q. Xin, Appl. Catal. A—Gen. 167 (1998) 39.
[5] J. Kaspar, P. Fornasiero, M. Graziani, Catal. Today 52 (1999) 285.
[6] Y.M. Xu, C.H. Langford, J. Phys. Chem. 99 (1995) 11501.
[7] X.T. Gao, S.R. Bare, J.L.G. Fierro, I.E. Wachs, J. Phys. Chem. B 103 (1999) 618.
[8] S. Zhang, L. Gao, Q.H. Zhang, J. Sun, J. Solid State Chem. 162, (2001) 138, doi:10.1006/jssc.2001. 9373.
[9] J. Fung, I. Wang, J. Catal. 130 (1991) 577.
[10] V.M. Mastikhin, V.V. Terskikh, O.B. Lapina, S.V. Filimonova, M. Seidl, H. Knozinger, J. Catal. 156 (1995) 1, doi:10.1006/jcat.1995. 1225.
[11] H.K. Matralis, M. Ciardelli, M. Ruwet, P. Grange, J. Catal. 157, (1995) 368, doi:10.1006/jcat.1995. 1302.
[12] J. Ramirez, A. Gutierrez-Alejandre, J. Catal. 170, (1997) 108, doi:10.1006/jcat.1997. 1713.
[13] Y. Xie, Y. Tang, Adv. Catal. 37 (1990) 1.
[14] Y.L. Fu, Y. Tian, P. Lin, J. Catal. 132 (1991) 85.
[15] J.C. Otamiri, S.L.T. Andersson, A. Andersson, Appl. Catal. 65 (1990) 159.
[16] F.P.J.M. Kerkhof, J.A. Moulijn, J. Phys. Chem. 83 (1979) 1612.

[17] M. Wu, D.M. Hercules, J. Phys. Chem. 83 (1979) 2003.
[18] P. Larsson, A. Andersson, L.R. Wallenberg, B. Svensson, J. Catal. 163, (1996) 279, doi:10.1006/jcat.1996. 0331.
[19] L. Dong, Y.H. Hu, M.M. Shen, T. Jin, J. Wang, W.P. Ding, Y. Chen, Chem. Mater. 13 (2001) 4227.
[20] T.J. Dines, C.H. Rochester, A.M. Ward, J. Chem. Soc., Faraday Trans. 87 (1991) 1611.
[21] K.Y.S. Ng, E. Gulari, J. Catal. 92 (1985) 340.
[22] G.A. Schuit, B.C. Gates, A.I.Ch.E. J. 19 (1993) 417.
[23] L.F. Zhang, Y. Chen, Catal. Lett. 12 (1992) 51.
[24] M.A. Stranick, M. Houalla, M.D. Hercules, J. Catal. 106 (1987) 362.
[25] W.P. Dow, Y.P. Wang, T.J. Huang, J. Catal. 160 (1996) 155, doi:10.1006/jcat.1996. 0135.
[26] M. Fernandez-Garcia, C. Marquez-Alvarez, I. Rodriquez-Ramos, A. Guerrero-Ruiz, G.L. Haller, J. Phys. Chem. 99 (1995) 16380.
[27] Y. Chen, L.F. Zhang, J.F. Lin, Y.S. Jin, Catal. Sci. Technol. 1 (1991) 291.
[28] W.S. Xia, H.L. Wan, Y. Chen, J. Mole. Catal. A—Gen. 138 (1999) 185.
[29] B. Xu, L. Dong, Y. Chen, J. Chem. Soc., Faraday Trans. 94 (1998) 1905.
[30] P.A. Sermon, K. Rollins, P.N. Reyes, S.A. Lawrence, M.A. Martin Luengo, M.J. Davies, J. Chem. Soc., Faraday Trans. I 83 (1987) 1347.
[31] M. Del Arco, A. Caballero, P. Malet, V. Rives, J. Catal. 113 (1988) 120.
[32] G.C. Bond, S.N. Namijo, J.S. Wakeman, J. Mol. Catal. 64 (1991) 305.
[33] F.S. Delk II, A. Vavere, J. Catal. 85 (1984) 380.
[34] H.W. Chen, J.M. White, J.G. Ekerdt, J. Catal. 99 (1986) 293.
[35] M. Fernandez-Garcia, E. Gomez Rebollo, A. Guerrero Ruiz, J.C. Conesa, J. Soria, J. Catal. 172, (1997) 146, doi:10.1006/jcat. 1997.1842.
[36] H.Y. Huang, R.Q. Long, R.T. Yang, Appl. Catal. B—Evn 33 (2001) 127.